

Influence of Fe-clustering in the water oxidation performance of two-dimensional layered double hydroxides

Alvaro Seijas-Da Silva,^{‡a} Víctor Oestreicher,^{‡a} Eugenio Coronado^a and Gonzalo Abellán^{*a}

^aInstituto de Ciencia Molecular (ICMol), Universitat de València, Catedrático José Beltrán 2, 46980, Paterna,
Valencia, Spain.

[‡]Both authors contributed equally to this work.

*gonzalo.abellan@uv.es

Table of content

Figure S1. UV-Vis spectra of aqueous solutions containing $[\text{Fe(III)}] = 5 \text{ mM}$ without and with $[\text{TEA}] = 5 \text{ mM}$.

Figure S2. High resolution Mg 1s XPS spectra in the range 1315 – 1295 eV for samples MgFe-TEA and MgFe.

Figure S3. High resolution Cl 2p XPS spectra in the range 210 – 190 eV for samples MgFe-TEA and MgFe.

Table S1. Chemical formula, structural parameters (d), crystalline size (L), Mg:Fe and Cl:Fe ratios for MgFe and MgFe-TEA LDHs samples.

Figure S4. Fitting of the $1/\chi_M$ to a Curie–Weiss law for samples MgFe-TEA and MgFe.

Table S2. Magnetic parameter of MgFe-TEA and MgFe samples.

Figure S5. Differences in the overpotential for both samples ($OP_{\text{MgFe}} - OP_{\text{MgFe-TEA}}$) as a function of the current density.

Figure S6. Electrochemical surface area (ECSA) of the MgFe-LDHs samples calculated from CVs performed in a non-faradaic region at different scan rates.

Figure S7. Electrocatalysts activation process performed as cyclic voltammetries recorded at 100 mV/s during 20 cycles: first cycle (shading cycle) and last cycle (thick line).

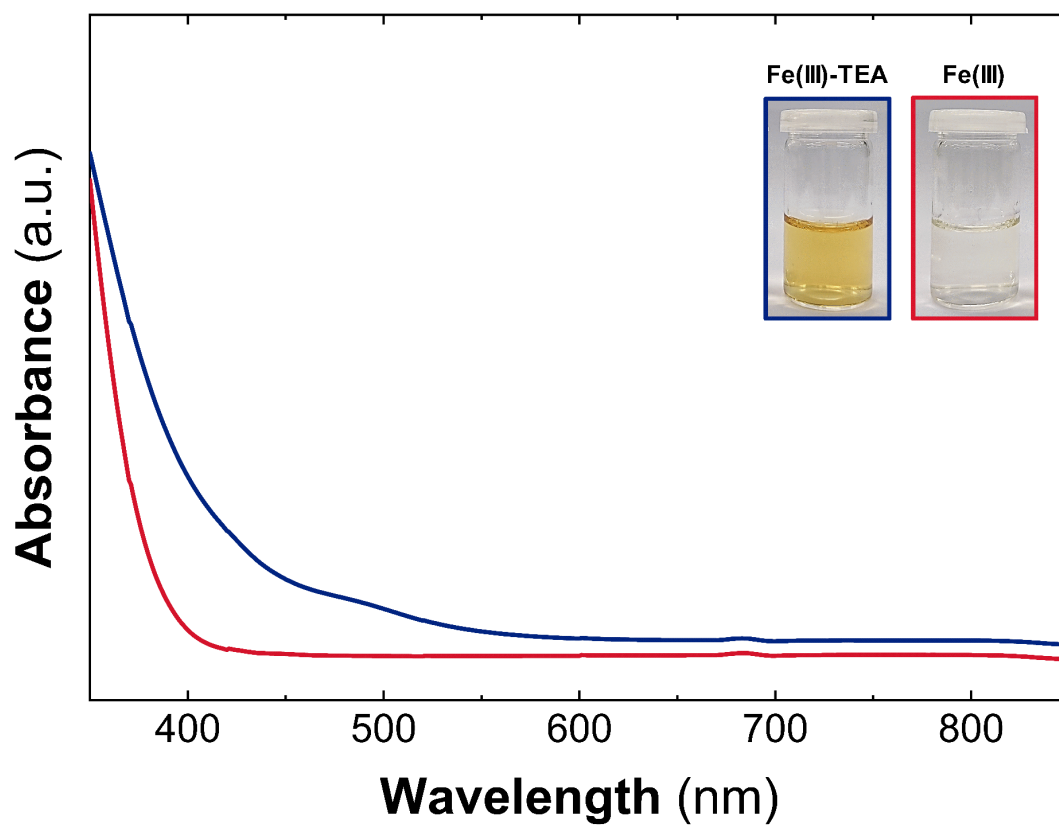


Figure S1. UV-Vis spectra of aqueous solutions containing $[\text{Fe(III)}] = 5 \text{ mM}$ without (red) and with $[\text{TEA}] = 5 \text{ mM}$ (blue).

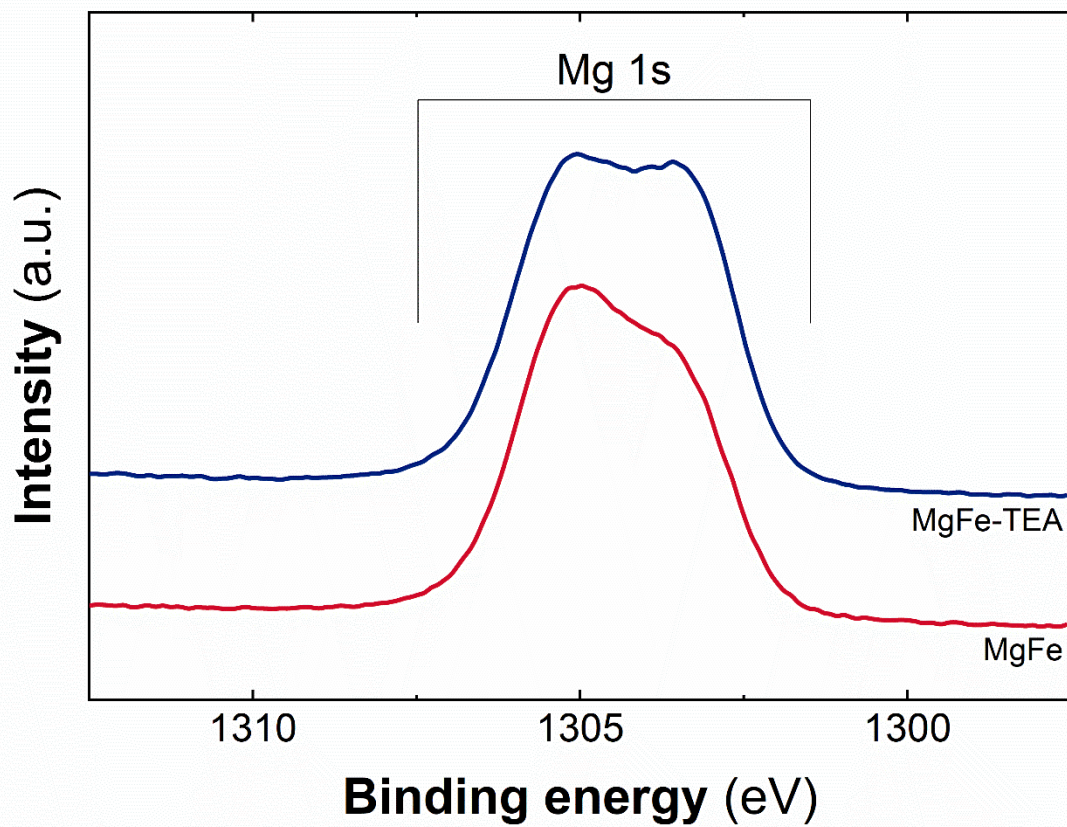


Figure S2. High resolution Mg 1s XPS spectra in the range 1315 – 1295 eV for samples MgFe-TEA (blue) and MgFe (red).

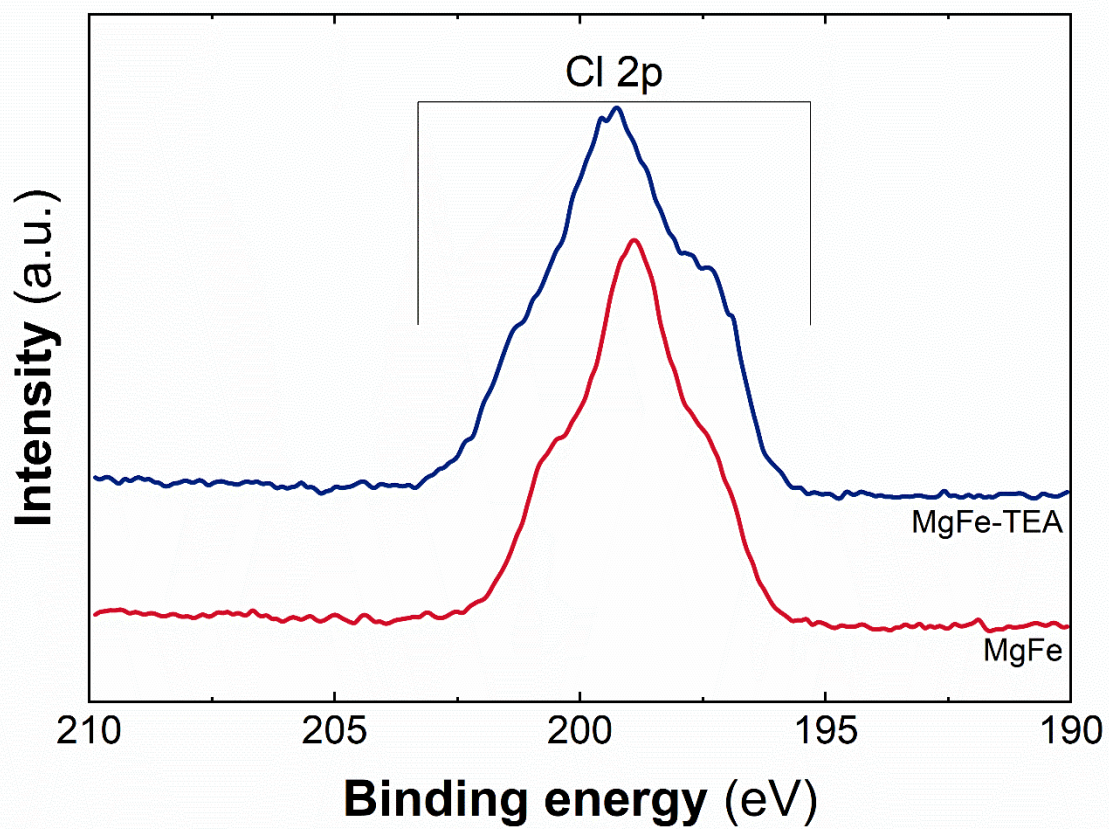


Figure S3. High resolution Cl 2p XPS spectra in the range 210 – 190 eV for samples MgFe-TEA (blue) and MgFe (red).

Table S1. Chemical formula, structural parameters (**d**), crystalline size (**L**), Mg:Fe and Cl:Fe ratios for MgFe and MgFe-TEA LDHs samples.

Sample	Chemical formula	d_{BS} (Å)	L_{001} (nm)	d_{110} (Å)	L_{110} (nm)	Mg:Fe			Cl:Fe	
						XPS	EDS	ICP-MS	XPS	EDS
MgFe-TEA	$Mg_2Fe(OH)_6Cl_{0.6}(CO_3)_{0.2} \cdot 0.5(H_2O)$	8.06	26.4	1.56	26.2	1.8	2.0	2.1	0.7	0.6
MgFe	$Mg_2Fe(OH)_6Cl_{0.6}(CO_3)_{0.2} \cdot 0.5(H_2O)$	8.06	18.5	1.56	27.2	1.7	1.9	2.1	0.7	0.6

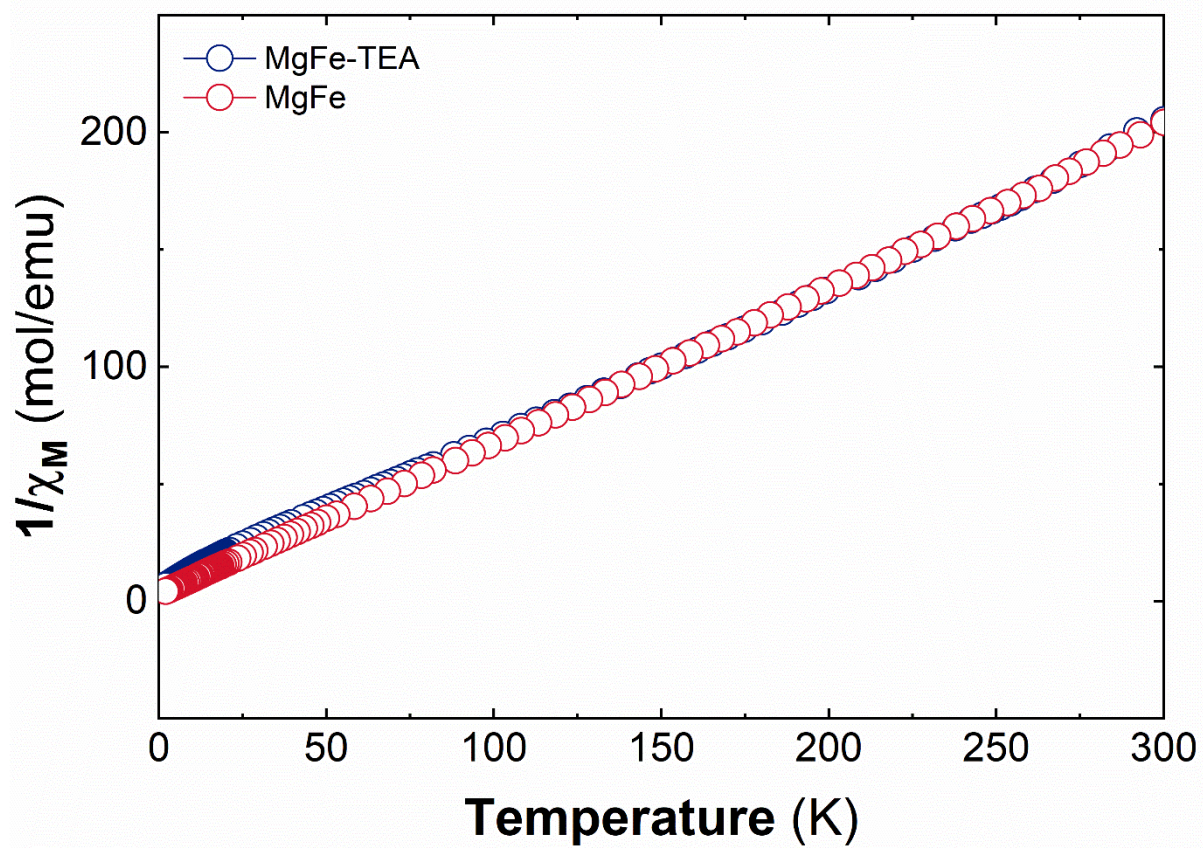


Figure S4. Fitting of the $1/\chi_M$ to a Curie–Weiss law for samples MgFe-TEA (blue) and MgFe (red).

Table S2. Magnetic parameters of MgFe-TEA and MgFe samples.

Sample	$C_{\text{spin-only}}$ (emu·K/mol)	C_{exp} (emu·K/mol)	Θ (K)
MgFe-TEA	1.44	1.44	-8.13
MgFe	1.44	1.45	-5.49

$C_{\text{spin-only}}$: expected spin-only value of the Curie constant, calculated as a diluted combination of Mg^{2+} ($S=0$) and Fe^{3+} ($S=5/2$).

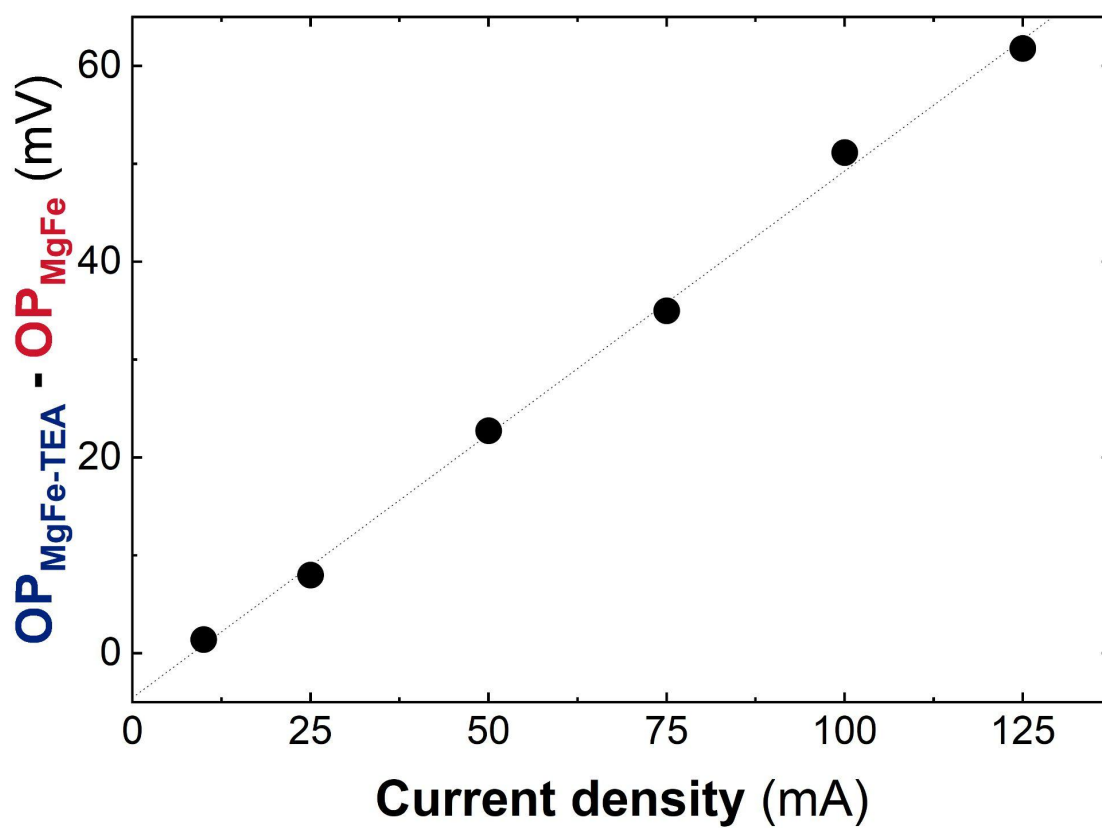


Figure S5. Differences in the overpotential for both samples ($OP_{MgFe} - OP_{MgFe-TEA}$) as a function of the current density.

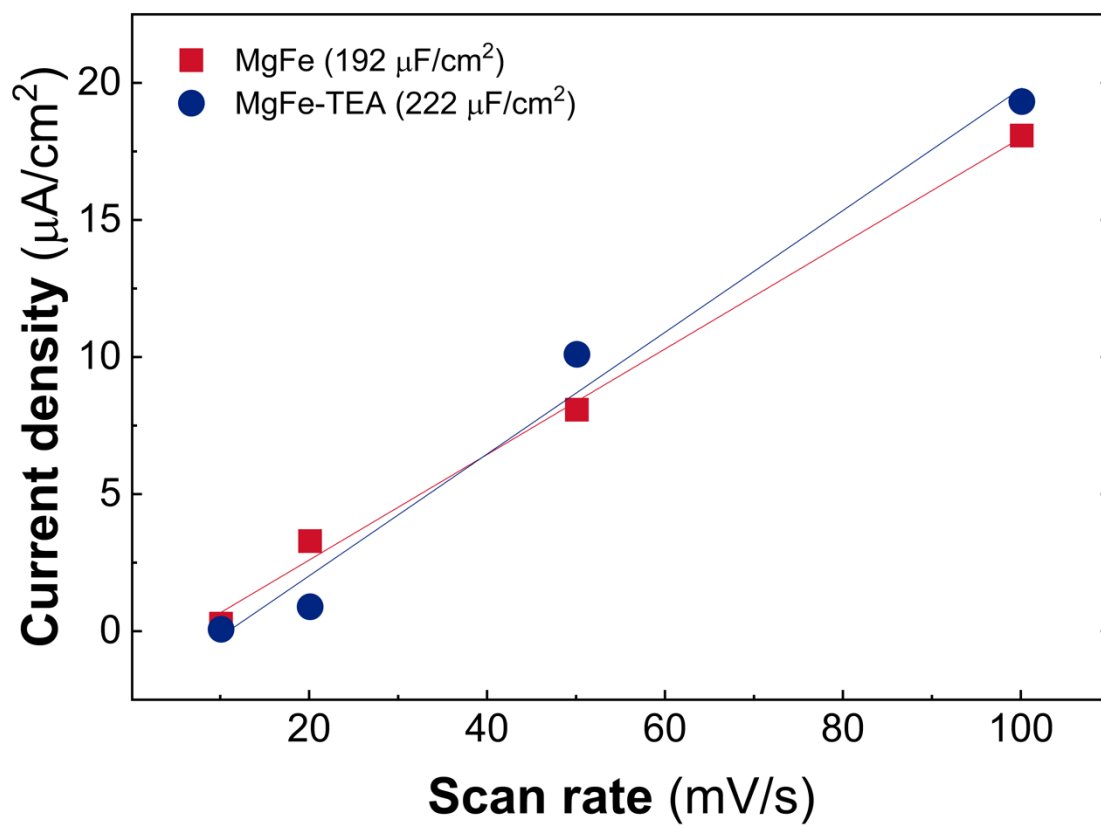


Figure S6. Electrochemical surface area (ECSA) of the MgFe-LDH samples calculated from CVs performed in a non-faradaic region at different scan rates.

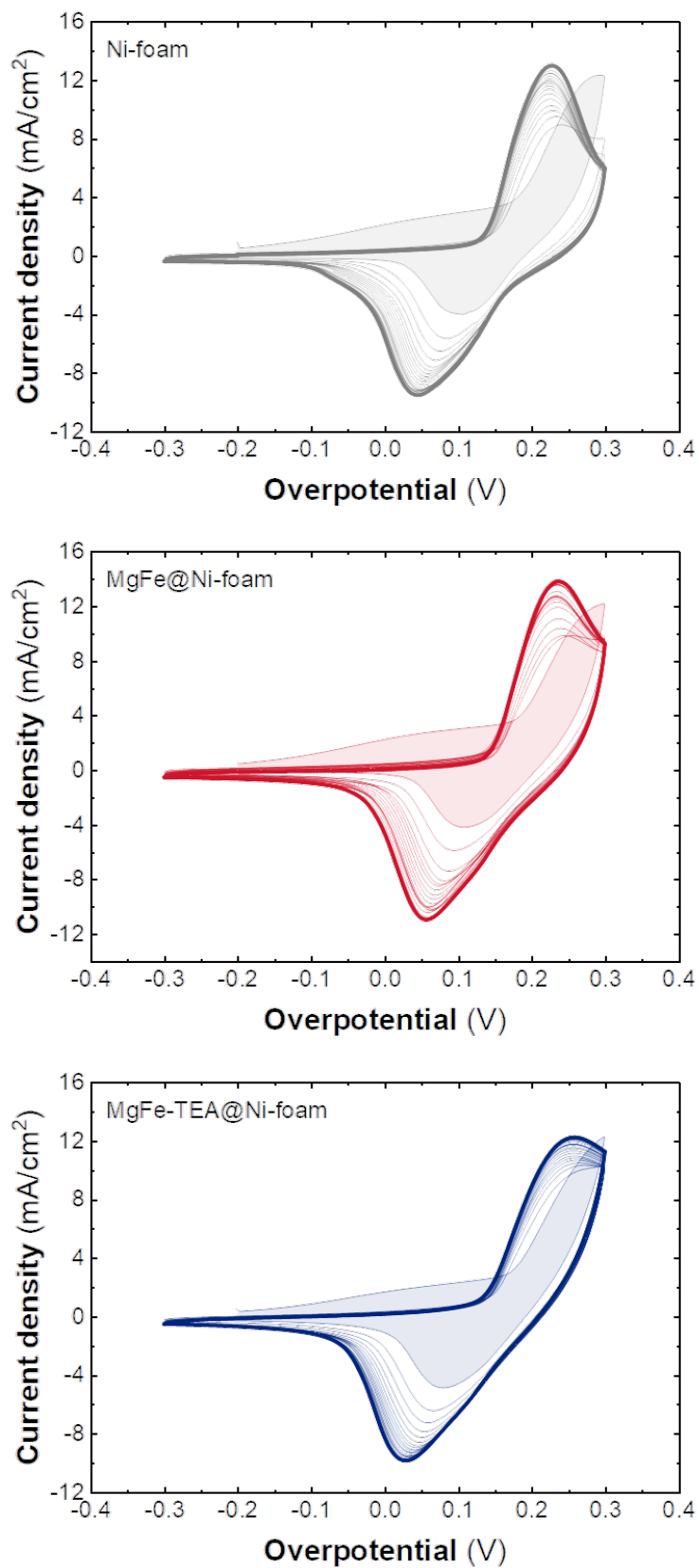


Figure S7. Electrocatalysts activation process performed as CVs recorded at 100 mV/s during 20 cycles: first cycle (shading cycle) and last cycle (thick line).